

Hierarchical generalization of dual unitarity

Xie-Hang Yu, Zhiyuan Wang, and Pavel Kos

Max-Planck-Institut für Quantenoptik, Hans-Kopfermann-Str. 1, 85748 Garching, Germany

(Dated: August 4, 2023)

Quantum dynamics with local interactions in lattice models display rich physics, but is notoriously hard to study. Dual-unitary circuits allow for exact answers to interesting physical questions in clean or disordered one- and higher-dimensional quantum systems. However, this family of models shows some non-universal features, like vanishing correlations inside the light-cone and instantaneous thermalization of local observables. In this work we propose a generalization of dual-unitary circuits where the exactly calculable spatial-temporal correlation functions display richer behavior, and have non-trivial thermalization of local observables. This is achieved by generalizing the single-gate condition to a hierarchy of multi-gate conditions, where the first level recovers dual-unitary models, and the second level exhibits these new interesting features. We also extend the discussion and provide exact solutions to correlators with few-site observables and discuss higher-orders, including the ones after a quantum quench. In addition, we provide exhaustive parametrizations for qubit cases, and propose a new family of models for local dimensions larger than two, which also provides a new family of dual-unitary models.

I. INTRODUCTION

One of the pivotal problems in quantum many-body physics is understanding the dynamics of extended systems with local interactions. Although the local interactions are simple, they generate complex dynamics, which is in general too hard to describe. The dynamics can be characterized with different probes such as local correlation functions, entanglement spreading, and other quantum information quantities. The understanding of this type of dynamics is currently at the center of attention in many fields spanning from nonequilibrium statistical mechanics, quantum information, condensed matter to high-energy physics and quantum gravity.

However, the complexity of quantum dynamics, both analytically and numerically, presents a significant hurdle. For example, the bond dimension of Matrix Product States (MPS) typically increases exponentially due to the linear growth in entanglement entropy [1, 2]. This necessitates the use of solvable models to unravel many-body behavior. The most well-known examples are non-interacting (Gaussian) systems such as free fermions or bosons, Clifford circuits, and Bethe-ansatz interacting integrable models [3]. Unfortunately, all of these models are not chaotic, in contrast to generic examples. If one is prepared to average over an ensemble of systems, random unitary circuits [4] provide examples of solvable chaotic dynamics. However, the averaged results miss a lot of relevant physics and are less relevant for translationally invariant systems.

A recently discovered solvable family of models, known as *dual-unitary* quantum circuits [5], has distinctly different solvable structure which does not require averaging, and moreover contains both integrable and chaotic examples. The basic property, which enables solvability is the unitarity of the local gates in the space direction. In this paper, we generalize this to a condition on a few gates and unravel new families of solvable models.

Dual unitarity was shown to enable analytical com-

putations of correlation functions [5, 6], chaos indicator spectral form factor [7, 8], operator and entanglement spreading [6, 9–15], deep thermalization through emergent state designs [16–18], study of eigenstate thermalization [19] and temporal entanglement [20–22]. They also proved useful in connections with measurement induced phase transitions [23–25], had aspects of their computational power characterized [26], and have already been realized in experimental setups [27, 28]. The exhaustive parametrization is simple and is known for dual-unitary gates of two qubits [5]. In general, however, only certain non-exhaustive families of gates are known [29–36]. Some extension of the dual-unitary condition were already proposed. One can add arbitrary perturbations and perform a perturbative analysis [37, 38], generalize to the case of having three or more unitary directions [35, 39, 40], study random and holographic geometries [41, 42], and lift the ideas to open systems [43] and classical symplectic circuits [44].

Despite the success of the dual-unitary circuits (and its extension) in describing physical properties of non-equilibrium dynamics, they exhibit some non-universal features. Firstly, in dual-unitary circuits the non-vanishing correlation functions exist only on light-cones edges. Secondly, the thermalization of local observables is instantaneous. The fundamental reason behind these non-universal features is that their single gate’s conditions are too restrictive. In fact, this family of models doesn’t even include many gates that are solvable by other methods, e.g. the Identity, Controlled-Not and Controlled-Z. This raises the question: Can the dual-unitary condition be relaxed to allow for richer physics while still maintaining the solvability of the spatial-temporary correlation function?

In this paper, we answer these questions in the affirmative by relaxing the dual-unitary condition and extending it to a hierarchy of conditions that contains more and more local gates. The dual-unitary condition on one gate forms the the first level of the Hierarchy denoted by \mathcal{L}_1 ,

whereas the circuit with two-gate condition at the second level of the Hierarchy \mathfrak{L}_2 allows for the exact calculation of two-point correlation functions, which are richer than for dual unitaries, i.e. non-vanishing at the same site and different times. Moreover, when quenched from the solvable initial states, the \mathfrak{L}_2 circuit exhibits non-trivial thermalization of local observables. We go beyond \mathfrak{L}_2 and show that higher levels of hierarchical circuits limit the maximum speed of information spreading.

We provide complete parameterization for the \mathfrak{L}_2 and \mathfrak{L}_3 circuits in the qubit case. For the larger local Hilbert space dimensions, we propose a new method to construct a class of circuits using the Clifford group that is analytically trackable. This method can also be used to construct new families of dual-unitary circuit.

The paper is structured as follows: In Sec. II, we introduce the notation. Subsec. II A reviews the dual-unitary circuits and introduces our parametrization method using Clifford groups. The hierarchical generalization is outlined in subsec. II B. After that, we dive into details of the \mathfrak{L}_2 and \mathfrak{L}_3 circuits in subsecs. II C and II D, including their parametrization. In Sec. III, we discuss the physical applications of the different levels of Hierarchical circuits. Subsec. III A considers the two-point correlation functions for \mathfrak{L}_1 , \mathfrak{L}_2 and \mathfrak{L}_3 circuits. In subsec. III B, we extend our discussion to the correlation functions of multisite observables, and three-point correlation functions. Subsec. III C discusses the evolution of an initial state from a quantum quench. We generalize the solvable initial states [6] for the \mathfrak{L}_2 circuit and explore the relationship between quench dynamics and quantum thermalization. In Sec. IV, we summarize the main results of the paper and discuss future directions.

II. HIERARCHICAL GENERALIZATION OF DUAL UNITARITY

In this paper we consider a chain comprised of L cells, with each cell containing 2 sites at integers and odd-half integer sites. At each site there is a Hilbert space with a local dimension D . Consequently, the corresponding total Hilbert space is $\mathcal{H} = (C^D)^{2L}$. The local basis is denoted by $|j\rangle$ with $j = 0, 1, \dots, D-1$. The chain's dynamics is governed by a brickwall Floquet circuit

$$\mathbb{U} = \mathbb{T}_{2L} u^{\otimes L} \mathbb{T}_{2L}^\dagger u^{\otimes L}$$

where \mathbb{T}_{2L} is a periodic translation operator on $2L$ sites, and u a local gate. Here, for simplicity, we assume translational invariance of the circuit and introduce periodic boundary conditions. However, our result can be easily generalized to non-uniform cases and open boundary conditions. Above, we graphically represented local unitary

gates with dimension $D^2 \times D^2$ by a box with incoming and outgoing legs,

$$u = \begin{array}{c} \diagup \\ \square \\ \diagdown \end{array}, \quad u^\dagger = \begin{array}{c} \diagdown \\ \square \\ \diagup \end{array}, \quad (1)$$

satisfying unitarity conditions

$$\begin{array}{c} uu^\dagger \\ u^\dagger u \end{array} = \begin{array}{c} \diagup \\ \square \\ \diagdown \\ \diagup \\ \square \\ \diagdown \end{array} = \begin{array}{c} | \\ | \\ | \\ | \end{array} = I_{D^2}, \quad (2)$$

Our results can be more succinctly expressed in the folded picture, where an operator over $(C^D)^{2L}$ is vectorized to a vector in $(C^D)^{4L}$ by the linear map on the basis

$$|m\rangle \langle n| \rightarrow |m\rangle |n\rangle. \quad (3)$$

The time evolution in Schrodinger picture can also be vectorized to

$$u()u^\dagger \rightarrow u \otimes u^*. \quad (4)$$

Graphically, u^\dagger is folded back behind u , thereby forming a joint operator $w \equiv u \otimes u^*$. It is also convenient to denote the vectorized identity operator in the folded picture as an empty bullet $|\circ\rangle = \frac{1}{\sqrt{D}} |I_D\rangle$, which is shown below

$$w = \begin{array}{c} \diagup \\ \square \\ \diagdown \end{array} = \begin{array}{c} \diagup \\ \square \\ \diagdown \\ \diagup \\ \square \\ \diagdown \end{array}, \quad \circ = \frac{1}{\sqrt{D}} \begin{array}{c} \diagup \\ \square \\ \diagdown \end{array}. \quad (5)$$

With these notations, the unitarity condition (2) is graphically expressed as $\begin{array}{c} \diagup \\ \square \\ \diagdown \end{array} \circ = \begin{array}{c} \circ \\ | \\ | \end{array}$ and $\begin{array}{c} \circ \\ | \\ | \end{array} = \begin{array}{c} \diagup \\ \square \\ \diagdown \end{array} \circ$.

A. Dual Unitarity

Understanding the dynamics of extended locally interacting systems is at the core of quantum many-body physics. However, this problem is usually analytically intractable and numerically exponentially hard. To make progress, we need some additional structure. One possibility is to demand the so-called dual-unitarity condition [5] mentioned in the introduction, which enables various exact calculations even for chaotic dynamics.

Dual unitarity demands that the gate u is unitary even if we exchange the roles of space and time. This switching corresponds to changing which are input and output legs of the gate, resulting in the dual local gate \tilde{u} . It is formally introduced by reshuffling the indices

$$\tilde{u} = \begin{array}{c} \diagdown \\ \square \\ \diagup \end{array}, \quad \langle j | \langle l | \tilde{u} | i \rangle | k \rangle = \langle k | \langle l | u | i \rangle | j \rangle. \quad (6)$$

A gate is dual-unitary [5] if both u and \tilde{u} are unitary, so in addition to (2) we also require

$$\tilde{u}^\dagger \tilde{u} = \tilde{u} \tilde{u}^\dagger = I_{D^2}, \quad (7)$$

which in the folded graphical language yields

$$\begin{array}{c} \text{---} \circ \text{---} \\ \diagup \quad \diagdown \\ \text{---} \circ \text{---} \end{array} = \begin{array}{c} \text{---} \circ \text{---} \\ \text{---} \circ \text{---} \end{array}, \quad \begin{array}{c} \text{---} \circ \text{---} \\ \diagdown \quad \diagup \\ \text{---} \circ \text{---} \end{array} = \begin{array}{c} \text{---} \circ \text{---} \\ \text{---} \circ \text{---} \end{array}. \quad (8)$$

The family of models defined in this way encompasses free, interacting integrable and chaotic models [5]. The parametrization of dual-unitary gates for $D = 2$ has been fully determined [5]. Despite a lack of the complete parametrization of dual-unitary gates for $D \geq 3$, several families have been proposed [29–34]. We proceed to add another family to the list, resulting in a novel extensive family of dual-unitary gates in higher dimensions. This parametrization also proves useful when addressing the hierarchical generalization of dual-unitary circuits in the following sections.

Consider the following parametrized family of two-qudit unitary gates:

$$u = (v_1 \otimes v_2) u_0 (v_3 \otimes v_4), \quad (9)$$

where v_1, v_2, v_3, v_4 are single site unitary gates, and u_0 is defined as

$$u_0 = \sum_{0 \leq p, q \leq D-1} \theta_{p,q} |\psi_{p,q}\rangle \langle \psi_{p,q}|. \quad (10)$$

Here $\{\theta_{p,q}\}_{0 \leq p, q \leq D-1}$ is a collection of $U(1)$ phases, and $\{|\psi_{p,q}\rangle\}_{0 \leq p, q \leq D-1}$ is an orthonormal basis for the 2-qudit Hilbert space $(\mathbb{C}^D)^2$ defined as

$$|\psi_{p,q}\rangle \equiv \frac{1}{\sqrt{D}} \sum_{1 \leq i, j \leq D} (\tau^p \sigma^q)_{ij}^* |i\rangle \otimes |j\rangle, \quad (11)$$

where σ, τ are the $D \times D$ dimensional generators of the Clifford group satisfying the relations

$$\sigma^D = \tau^D = 1, \quad \sigma\tau = \omega\tau\sigma, \quad (12)$$

with $\omega = e^{2\pi i/D}$ a D -th root of unity. The matrices σ, τ generate the full matrix algebra $M_D(\mathbb{C})$, and we can always choose σ to be diagonal and τ to be real. Explicitly, they are defined as

$$\begin{aligned} \sigma &= \sum_{j=0}^{D-1} \omega^j |j\rangle \langle j|, \\ \tau &= \sum_{j=0}^{D-1} |j+1\rangle \langle j|, \end{aligned} \quad (13)$$

where $|D\rangle \equiv |0\rangle$. Related parametrization in terms of Operator-Schmidt decomposition appeared in [45]. We report a novel more general framework in Appendix A, but we don't include it here, since we don't need it in the following analysis.

We proceed to investigate conditions on the parameters $\{\theta_{p,q}\}_{0 \leq p, q \leq D-1}$ for u to be a dual-unitary gate. After a space-time reshuffling of indices defined in Eq. (6), we have $\tilde{u} = (v_4^T \otimes v_2) \tilde{u}_0 (v_3 \otimes v_1^T)$, where

$$\tilde{u}_0 = \frac{1}{D} \sum_{0 \leq p, q \leq D-1} \theta_{p,q} \tau_{p,q} \otimes \tau_{p,q}^*, \quad (14)$$

with $\tau_{p,q} \equiv \tau^p \sigma^q$. Then the unitarity condition (7) on \tilde{u} is equivalent to

$$\sum_{0 \leq p, q, r, s \leq D-1} \theta_{p,q}^* \theta_{r,s} \tau_{p,q}^\dagger \tau_{r,s} \otimes \tau_{p,q}^T \tau_{r,s}^* = D^2 \tau_{0,0} \otimes \tau_{0,0}. \quad (15)$$

Notice that the single site unitary gates v_1, v_2, v_3, v_4 do not appear in the above expression. We simplify Eq. (15) further with the following relations satisfied by $\tau_{p,q}$

$$\begin{aligned} \tau_{p,q} \tau_{r,s} &= \omega^{qr} \tau_{p+r, q+s}, \\ \tau_{p,q}^* &= \tau_{p,-q} \\ \tau_{p,q}^T &= \omega^{-pq} \tau_{-p, q}. \end{aligned} \quad (16)$$

They follow from Eqs. (12) and (13) by straightforward computation. Simplifying Eq. (15) using Eq. (16), and comparing the coefficients of both sides using the fact that $\{\tau_{p,q}\}_{0 \leq p, q \leq D-1}$ forms a basis of the matrix algebra $M_D(\mathbb{C})$, we obtain

$$\sum_{0 \leq p, q \leq D-1} \theta_{p,q}^* \theta_{p+k, q+l} = 0, \quad \text{for } (k, l) \neq (0, 0). \quad (17)$$

In this way, the original dual unitarity condition, which involves $2D^4$ equations and $2D^4 - 1$ real unknowns simplifies to a set of $D^2 - 1$ equations with $D^2 - 1$ real unknowns (notice that we can set $\theta_{0,0} = 1$ without loss of generality). A simple yet nontrivial ansatz for $\theta_{p,q}$ is ¹

$$\theta_{p,q} = \omega^{\lambda p^2 + \mu pq + \nu q^2}, \quad (18)$$

where $\mu \in \mathbb{Z}$, and $\lambda, \nu \in \mathbb{Z}$ if D is odd while $\lambda, \nu \in \mathbb{Z}/2$ if D is even (which guarantees that $\theta_{p,q}$ is periodic both in p and q with period D). This ansatz also results in the perfect tensors in odd dimensions which are found in [32]. Inserting the ansatz (18) into Eq. (17), we see that dual-unitarity requires that $k = l = 0$ is the only solution to the following system of equations ²

$$\begin{aligned} 2\lambda k + \mu l &= 0 \pmod{D}, \\ \mu k + 2\nu l &= 0 \pmod{D}. \end{aligned} \quad (19)$$

For example, when $D = 3$, $\lambda = \mu = 1, \nu = -1$ satisfies this condition. In later sections we will use the ansatz Eq. (10) and Eq. (18) to find examples of hierarchical generalizations of dual-unitary gates.

In this subsection we recapped the basics of dual-unitarity and introduced a novel family of dual-unitary models for $D > 2$. A particular subset of solutions from this family appeared before in [34]. This leaves us in a good position to introduce the generalization in the next subsection.

¹ A particularly simple solution to Eq. (17) is $\theta_{p,q} = \theta_{p+q} \omega^{p^2 + pq}$, where $\{\theta_p\}_{p=0}^{D-1}$ are arbitrary $U(1)$ phases. However, this family of dual-unitary gates are actually the same as those given in Eq. (25) of Ref. [34].

² A sufficient condition for this is that the determinant $4\lambda\nu - \mu^2$ is invertible modulo D .

B. Hierarchical Generalization

As mentioned in the Introduction, dual unitarity imposes conditions on only a single gate, which restricts the possible physical behaviours. It also excludes certain fundamental and well-known gates, such as the Identity and the Controlled-Not gate which are solvable yet not dual-unitary. To unveil more intricate quantum dynamics and include these Clifford gates in a more general notion of solvability, we define a *hierarchy of conditions*. This gives us new families of models.

Since only one green box plays a part in the dual-unitary condition (8), we will call dual-unitarity also the *first level of the Hierarchy* and denote it as \mathcal{L}_1 . In the subsequent subsections II C and II D, we extend the concept of dual unitarity (\mathcal{L}_1) to conditions involving two and three gates, resulting in the second level \mathcal{L}_2 and the third level \mathcal{L}_3 of the Hierarchy.

C. Second level of the Hierarchy

In this subsection, we introduce the gates from \mathcal{L}_2 , which are more general than dual-unitary gates. \mathcal{L}_2 contains CNOT and identity, as well as a large family of non-trivial gates whose dynamics cannot be solved by any previous techniques and reveals richer physics. The gates from this family fulfill a condition involving two gates, which is weaker than dual-unitary condition:

$$(20)$$

Algebraically, we can express the condition as

$$(I_D \otimes \tilde{u}^\dagger) \cdot \tilde{u}^\dagger \tilde{u} \otimes I_D \cdot (I_D \otimes \tilde{u}) = I_D \otimes \tilde{u}^\dagger \tilde{u},$$

$$(I_D \otimes \tilde{u}) \cdot \tilde{u} \tilde{u}^\dagger \otimes I_D \cdot (I_D \otimes \tilde{u}^\dagger) = I_D \otimes \tilde{u} \tilde{u}^\dagger. \quad (21)$$

A direct observation shows that if a circuit is \mathcal{L}_1 , it must be \mathcal{L}_2 . This, together with the fact that the identity is in \mathcal{L}_2 but not in \mathcal{L}_1 , implies that \mathcal{L}_1 is a proper subset of \mathcal{L}_2 : $\mathcal{L}_1 \subsetneq \mathcal{L}_2$. Next we focus on the gates that are in \mathcal{L}_2 but not in \mathcal{L}_1 , the set we denote as $\bar{\mathcal{L}}_2 = \mathcal{L}_2 - \mathcal{L}_1$.

Similarly to the \mathcal{L}_1 case [5], we will derive the complete parametrization of the $\bar{\mathcal{L}}_2$ for the qubits. When $D = 2$, an exhaustive parametrization of 2-qubit gates is

$$u = v_1 \otimes v_2 e^{i(J_x \sigma_x \sigma_x + J_y \sigma_y \sigma_y + J_z \sigma_z \sigma_z)} v_3 \otimes v_4. \quad (22)$$

Here σ_i are Pauli matrices and v_1, v_2, v_3, v_4 are all single site gates from $\mathbb{S}\mathbb{U}(2)$. We may simplify the gate structure by setting $v_3 = v_4 = I_D$ without any loss of generality³. The trivial example from $\bar{\mathcal{L}}_2$ is a tensor product of two single-site operators. Apart from that, the $\bar{\mathcal{L}}_2$ condition fixes $J_z = \frac{\pi}{4}, J_x = J_y = 0$ ⁴ and v_1, v_2 to be elements of the set

$$\{U(r, \theta, \phi) | \sqrt{2} \sin r \sin \theta = \pm 1\}, \quad (23)$$

where $U(r, \theta, \phi)$ is defined as $e^{ir(\cos \theta \sigma_z + \sin \theta (\cos \phi \sigma_x + \sin \phi \sigma_y))}$, representing a $\mathbb{S}\mathbb{U}(2)$ on the Bloch sphere. Geometrically, this specific combination of r, θ, ϕ represents a rotation that maps σ_z to the $x - y$ plane.

The dimension of $\bar{\mathcal{L}}_2$ can be counted as follows. Out of 12 parameters determining the 4 local $\mathbb{S}\mathbb{U}(2)$ gates, e.g. the Euler angles, two are redundant because the rotation around the z -axis commutes with the Ising interaction resulting from $J_z = \frac{\pi}{4}, J_x = J_y = 0$. Further, Eq. (23) provides 2 constraints. After considering the global phase, the total independent parameters to characterize a qubit $\bar{\mathcal{L}}_2$ circuit is $12 - 2 - 2 + 1$. Therefore, we have defined a new 9-dimensional family of solvable models which are not part of 12-dimensional set of \mathcal{L}_1 gates [33].

Note that the control not gate (CNOT) can be decomposed into the form of Eq. (22) as

$$v_1 = e^{-i\frac{\pi}{4}\sigma_z}, \quad v_2 = H\sigma_x \cdot e^{i\frac{\pi}{4}\sigma_z},$$

$$v_3 = I_2, \quad v_4 = \sigma_x H. \quad (24)$$

with $J_x = 0, J_y = 0, J_z = \frac{\pi}{4}$ and an addition global phase $e^{-i\frac{\pi}{4}}$. $H = \frac{1}{\sqrt{2}} \begin{pmatrix} 1 & 1 \\ 1 & -1 \end{pmatrix}$ is the Hadamard gate, and v_4 can be absorbed into v_1 . It is easy to check that the single site operator gate v_1 and v_2 satisfy (23).

In higher dimensions, we do not yet possess a complete parametrization for the \mathcal{L}_2 case. Nevertheless, we can discern two distinct and rich families. The first family is associated with generalized Controlled-NOT gate in higher dimension surrounded by 4 single site operators

$$u = v_1 \otimes v_2 C_\tau v_3 \otimes v_4, \quad (25)$$

with $C_\tau = \sum_i |i\rangle \langle i| \otimes \tau^i$. Following a similar argument as below Eq. (22), we set $v_3 = v_4 = I_D$. In this case, v_1 and v_2 must satisfy

$$\sum_j \langle j | v_1 | i \rangle \langle j + k' - k | v_1^* | i \rangle = \delta_{k, k'} \text{ for } \forall k, k', i.$$

$$\sum_j \langle i | v_2 | j \rangle \langle i | v_2^* | j + k' - k \rangle = \delta_{k, k'} \text{ for } \forall k, k', i. \quad (26)$$

These two equations share a symmetry of exchanging columns and rows between themselves.

The second family is derived using the Clifford group method from subsection II A. Utilizing the proposed ansatz from Eqs. (9) and (10), we set $v_3 = v_4 = I_D$ and simplify Eq. (21) to:

$$\begin{aligned}
& \left(\sum_b \theta_{p_b, q_b}^* \theta_{p_b+k, q_b+l} \right) \left(\sum_d \theta_{p_d, q_d}^* \theta_{p_d+s, q_d+t} \tau_{p_d, q_d}^\dagger v_1^* \tau_{k, -l} v_1^T \tau_{p_d, q_d} \right) = 0, \\
& \left(\sum_b \theta_{p_b, q_b}^* \theta_{p_b+k, q_b+l} \right) \left(\sum_d \theta_{p_d, q_d}^* \theta_{p_d+s, q_d+t} \tau_{-p_d, q_d}^\dagger v_2^* \tau_{-k, -l} v_2^T \tau_{-p_d, q_d} \right) = 0.
\end{aligned} \tag{27}$$

Here \sum_b is a shorthand for $\sum_{0 \leq p_b, q_b \leq D-1}$. The above equation should hold for $\forall (s, t) \neq (0, 0)$ and $(k, l) \neq (0, 0)$. If all terms in the first sum vanish separately, we obtain the \mathfrak{L}_1 . From these nonlinear equations, we can derive a family of $\bar{\mathfrak{L}}_2$, which is just one of the many possible solutions. The family is defined for $D = 4k + 2$ as

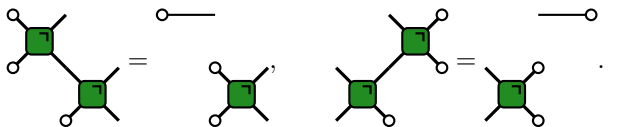
$$k \in \mathbb{N}^+ \text{ and } \theta_{p, q} = \omega^{\frac{Dpq}{2}}. \tag{28}$$

Another nontrivial example is given by

$$\theta_{p, q} = \begin{cases} \omega^{\frac{p^2}{2}} & D = \text{even} \\ \omega^{p^2} & D = \text{odd} \end{cases}, \tag{29}$$

In both of the two examples, the so far unspecified v_1 and v_2 belong a non-trivial subset of $\text{SU}(D)$. These subsets can be deduced from the second sums of Eq. (27). Different choices lead to both ergodic and non-ergodic dynamic.

Before concluding this subsection, we would like to highlight that Eq. (20) additionally implies

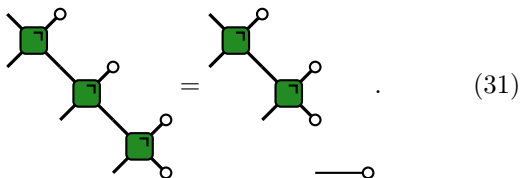


$$\tag{30}$$

The proof is shown in Appendix C. Eq. (30) will play an important role in computing the spatio-temporal correlation functions.

D. Third level of the Hierarchy

Following the principles from subsection II C, we define the third level hierarchical condition for \mathfrak{L}_3 as



$$\tag{31}$$

³ This is true because because v_1 at this time step can be combined with v_4 from the next time step, allowing for the redefinition $v_1 \rightarrow v_4 \cdot v_1$. This reasoning also applies to v_2 and v_3 .

⁴ The permutations among x, y, z also work.

An immediate observation reveals that a gate characterized as \mathfrak{L}_2 is also the \mathfrak{L}_3 . Nonetheless, we are again interested in the special subset of \mathfrak{L}_3 which does not belong to \mathfrak{L}_2 , designated as $\bar{\mathfrak{L}}_3 = \mathfrak{L}_3 - \mathfrak{L}_2$. A notable example within $\bar{\mathfrak{L}}_3$ is the controlled-Z gate.

We again use the complete parameterization of 2-qubit gates (22) and wlog set $v_3 = v_4 = I_2$. The condition defining $\bar{\mathfrak{L}}_3$ is satisfied either for all diagonal gates or for the case where $J_x = J_y = 0$ and any J_z with v_i satisfying $v_i = \cos \phi_i \sigma_x + \sin \phi_i \sigma_y$, $i \in 1, 2$.

To get some examples for $D > 2$, we use our Clifford gate parametrization method from Section II A. The algebraic equation of $\theta_{p, q}$ can be found in the Appendix B. To obtain some examples, we take the single-site operators v_i to be the identity. Some classes of the solutions obtained in this way are shown below.

$$\theta_{p, q} = \begin{cases} \omega^{p^2 + \frac{3}{2}q^2} & D = 12m + 2; \\ \omega^{p^2 + q^2} & D = 8m + 4; \\ \omega^{p^2 + \frac{3}{2}q^2} & D = 12m + 6, m \neq 1 \pmod{3}; \\ \omega^{p^2 + \frac{3}{2}q^2} & D = 12m + 10. \end{cases} \tag{32}$$

In principle, nothing stops us from going beyond the \mathfrak{L}_3 , by demanding even more general condition with even more gates. We expect the examples to be constructed in a similar way.

III. APPLICATIONS

A. Spatio-temporal correlator functions

In this subsection we focus on the spatio-temporal correlation functions, which are the most common objects to characterize the dynamics. In particular, they provide information about the thermalization and ergodicity of the system.

In most cases, the exact non-perturbative calculation of the spatio-temporal correlators is only available in free models and to some extent in interacting integrable ones [46–48]. Important progress has been made in understanding the correlations also in chaotic models, in particular dual-unitary (\mathfrak{L}_1) circuits which we extend here.

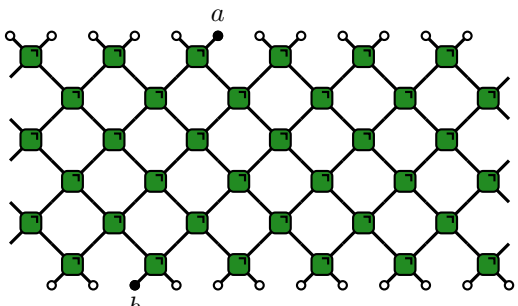
Due to the trivial propagation of an identity operator, we are only interested in the correlation function between two traceless Hilbert-Schmidt normalized operators a_i, b_j ⁵. Working in the Heisenberg picture, the

⁵ Hilbert Schmidt normalized means that $\text{Tr} a_i^\dagger a_i = 1$

spatio-temporal correlation function of normalized local operators can be expressed as

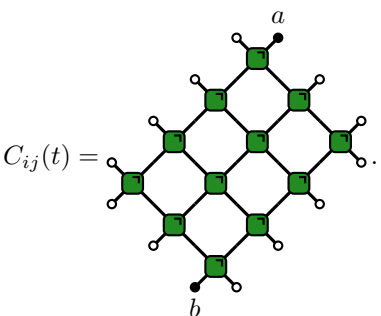
$$C_{ij}(t) = \langle a_i(t)b_j \rangle = D\text{Tr} \left((\mathbb{U}^t)^\dagger a_i \mathbb{U}^t b_j \frac{1}{D^{2L}} \right), \quad (33)$$

The factor $\frac{1}{D^{2L}}$ comes from the normalized infinite temperature state $\rho_\infty = \frac{I_{D^{2L}}}{D^{2L}}$. We also include a prefactor D in the definition to ensure that the autocorrelation function at time 0 is normalized to 1. Alternatively, this can be viewed as a quench from the $b_j \mathbb{1}$ state, i.e. b_j applied to the maximally mixed state. The correlations in the folded picture are graphically expressed as



$$C_{ij}(t) = \dots \quad (34)$$

Employing the time unitarity enables us to simplify the circuit from the bottom and top, yielding

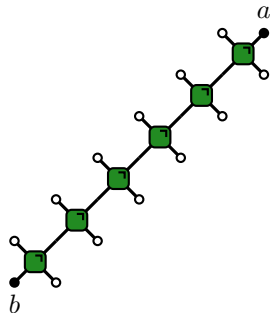


$$C_{ij}(t) = \dots \quad (35)$$

1. Dual unitarity

For completeness, here we briefly summarize the result for dual-unitary circuit from [5]. Intuitively, the time unitarity and space unitarity both determine a light cone outside which the correlation function vanishes. Therefore, correlators can solely manifest at the intersection of these two cones, forming a 1-dimensional straight line

that precisely bisects the temporal and spatial directions



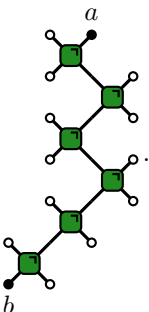
$$C_{ij}(t) = \dots \quad (36)$$

with other correlators vanishing. That other correlations vanish can be seen by repeatedly applying (8) to expression (35), which results in $\langle \circ | \bullet \rangle = 0$ since the operators a and b are traceless. In Eq. (36) each time step is just a quantum channel over $D \times D$ Hilbert space. Therefore, the correlators for the \mathfrak{L}_1 circuits can always be calculated efficiently and propagates only along two directions with maximal speed.

2. $\bar{\mathfrak{L}}_2$ circuits

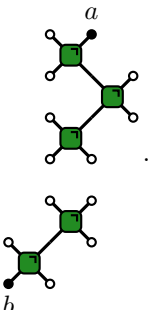
Moving beyond the \mathfrak{L}_1 , we are interested in which new features appear in the $\bar{\mathfrak{L}}_2$ circuits. Said differently, we are interested in what happens if the weaker condition (20) defining \mathfrak{L}_2 is satisfied but dual unitarity condition (8) is not.

We apply Eq. (20) to Eq. (35) and further simplify the circuit to



$$C_{ij}(t) = \dots \quad (37)$$

Lastly, Eq. (30) is utilised to address the corner of the path, leading to

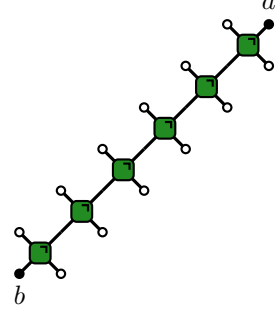


$$C_{ij}(t) = \dots \quad (38)$$

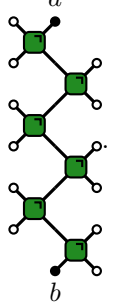
This correlator vanishes because the discontinuous path will be simplified to $\text{Tra}_i \text{Tr} b_j$ and both are traceless according to our assumption.

Therefore, the existence of nonvanishing correlators is limited to three possible directions, either at the light cone or at velocity zero.

$$C_{ij}(t) = \begin{array}{c} \text{Diagram 1} \\ \text{Diagram 2} \end{array}, \quad (39)$$

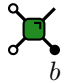
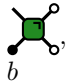
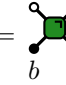
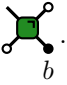


$$C_{ij}(t) = \begin{array}{c} \text{Diagram 2} \\ \text{Diagram 3} \end{array},$$



These expressions can be written using four single qudit channels:

$$\begin{array}{cc} \epsilon_L(b) = \text{Diagram 4} & \epsilon_R(b) = \text{Diagram 5} \\ M_L(b) = \text{Diagram 6} & M_R(b) = \text{Diagram 7} \end{array}, \quad (40)$$

To simplify the analysis, we assume j to be an integer, and the other case follows analogously. Thus

$$C_{ij}(t) = \begin{cases} \text{Tr}(aM_L^{2t}(b)) & t = i - j \\ \text{Tr}(a(\epsilon_R)^k(\epsilon_L\epsilon_R)^{\lfloor \frac{t}{2} \rfloor}(b)) & i = j, t = \mathbb{Z} + \frac{k}{2} \\ 0 & \text{otherwise} \end{cases} \quad (41)$$

This $C_{ij}(t)$ behaves differently than that in the dual-unitary case [5], as the circuits from \mathfrak{L}_2 allow for an additional non-vanishing direction along the time axis.

Let us mention here the connection with tri-unitaries circuits proposed in [39], where the correlation function also exclusively manifest in the same three directions. In fact, we can group the legs of two 2-qubit gates into a 3-qubit gates as

$$\text{Diagram 8} \Rightarrow \text{Diagram 9}. \quad (42)$$




However, in the tri-unitary case, the condition is

$$\text{Diagram 10} = \text{Diagram 11} \quad (43)$$



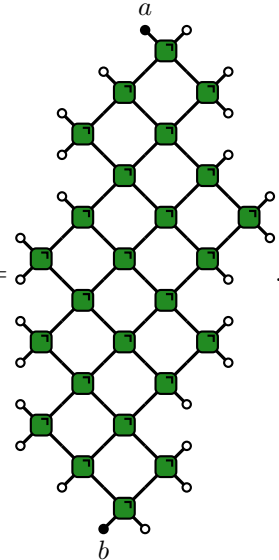

which is a much stronger condition than Eq. (20).

Interestingly, in the context of qubits ($D = 2$), it is impossible to observe all in principle allowed physical behaviors. The correlations along the light rays vanish since channels ϵ_L and ϵ_R correspond to the total depolarizing channel. Nevertheless, when $D > 2$, there are examples manifesting all of the properties discussed above, i.e. nonvanishing correlations in all three directions at all times. In other words, both the correlations in Eq. (39) are nontrivial. A such example is given in Eq. (28) which is also shown in Fig. 1(a). In this figure, the operator has support on two nearest neighbor sites, to eliminate the odd/even effect (for details see subsec. III B).

3. $\overline{\mathfrak{L}}_3$ and higher levels

In the case where the gate is classified as $\overline{\mathfrak{L}}_3$, the correlation function is reduced to

$$C_{ij}(t) = \text{Diagram 12}. \quad (44)$$

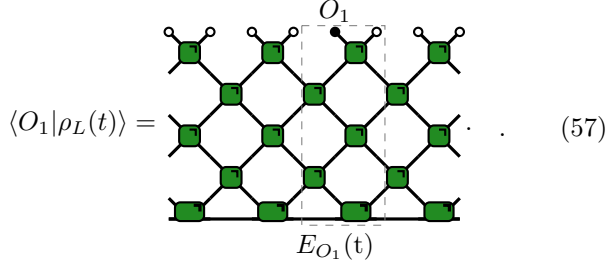


Intriguingly, this correlator does not vanish within the entire light cone, and no closed expression for it can be derived with a scaling polynomial in system size. Nevertheless, the hierarchical conditions influences the velocity of the light cone, slowing it down. As a general rule, for a k th level of Hierarchical circuit \mathfrak{L}_k , the velocity of the light cone will be suppressed to $\nu_k = \frac{k-2}{k}$.

B. Bigger operators and higher orders

In contrast to previous research, which concentrated primarily on correlators supported on a single site, exploring operators with multi-site support sheds light on

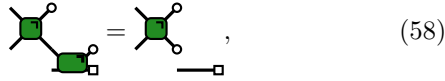
Here, $E(t) = E_{\perp}(t)$ and $E_{O_1}(t)$ are appropriate space transfer matrices



$$\langle O_1 | \rho_L(t) \rangle = \dots \quad (57)$$

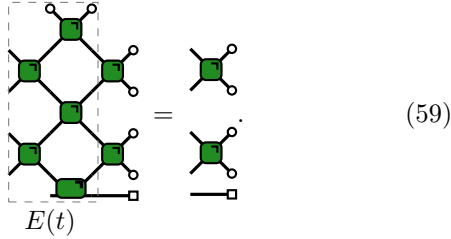
In this subsection we always assume periodic boundary conditions with large enough L such that the transfer matrix can be replaced by its fixed point.

If the initial state satisfies the following 1-point solvable condition for \mathfrak{L}_2




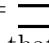
$$\dots \quad (58)$$


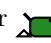
we can find an eigenstate of the transfer matrix with eigenvalue 1

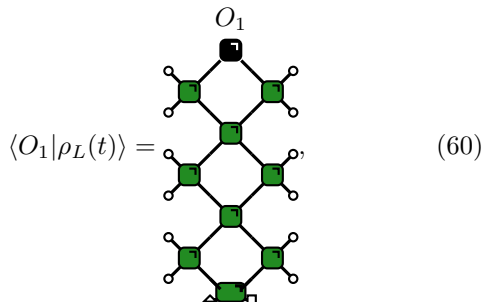


$$\dots \quad (59)$$

Since $\lim_{L \rightarrow \infty} \text{Tr}(\rho_L(t)) = 1$ due to the normalization, the largest eigenvalue of the transfer matrix must be 1 and non-degenerate. Therefore, the 1-point correlation function can be analytically calculated with this eigenvector.

It is worth to note that if the initial state satisfies the condition  = , Eq. (58) is automatically satisfied. This implies that we have identified a larger solvable class than both the pure solvable initial states for dual-unitary evolution [6] and in general mixed initial states for open 3-way unital evolution [43].

The correlation function for 2-site observables after a quench is very similar to Eq. (46). The only difference is the substitution of  at the base for .



$$\langle O_1 | \rho_L(t) \rangle = \dots \quad (60)$$

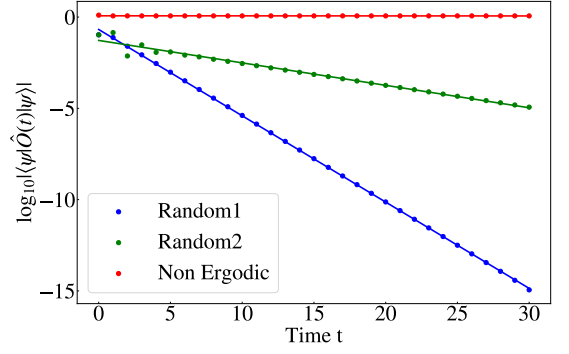


FIG. 3. The correlation function of a random two-site observable following a quantum quench starting from the Bell state $|\Psi_L\rangle$ defined in Eq. (62). The dynamics is governed by a \mathfrak{L}_2 circuit (symbols). We show its linear fit by solid lines. The blue and green data points show an exponential decay of the expectation value of observable, indicative of thermalization dynamics. In contrast, the red points remains constant at long times implying non-thermalization and non-ergodicity. The parameters for these three circuits can be found in Appendix D.

where $\langle \Delta |$ and $|\square\rangle$ are the left and right fixed points from Eq. (55). Following the same argument as in Sec. III B, the long time behavior is dictated by the largest eigenvalue of the quantum channel, \mathbb{Q} . The eigenspectrum of \mathbb{Q} can be completely deduced for qubits. Using the general parametrization of gates from \mathfrak{L}_2 in accordance with Eqs. (22) and (23), whereby $v_3 = v_4 = I$, $\theta_i = \arcsin \frac{1}{\sqrt{2} \sin r_i}$, $i \in \{1, 2\}$, only two non-zero eigenvalues, $\{1, \lambda\}$, exist. Eigenvalue 1 corresponds to the trivial eigenvector, i.e. identity and λ is given by

$$\lambda = \cos^2(\phi_2 - \phi_1) - 2(\sqrt{-\cos 2r_2 \cos r_1} + \sqrt{-\cos 2r_1 \cos r_2})^2. \quad (61)$$

Here r_1, r_2 are real numbers from the interval $[\frac{\pi}{4}, \frac{3\pi}{4}]$.

The dynamics is non-ergodic with $\lambda = 1$ if $\phi_1 = \phi_2 + 0, \pi$ and either $r_1 = \pi - r_2$ or $\cos 2r_1 = \cos 2r_2 = 0$. On the other hand, the circuit is non-ergodic also with $\lambda = -1$ if $\cos(\phi_1 - \phi_2) = 0$ and the last term in Eq. (61) equals 1, for example, by $r_1 = \frac{\pi}{2}, r_2 = \frac{\pi}{4}$. This gives all possible non-ergodic circuits for two-qubit gates from \mathfrak{L}_2 , apart from a tensor product of single-site gates. All other examples are ergodic and show exponential decay.

The most straightforward solution of initial states from Eq. (58) is the pure state with a bond dimension 1. One example is the qubit Bell state

$$|\Psi_L\rangle = \otimes_{k=1}^L \frac{|01\rangle_{2k-1, 2k} + |10\rangle_{2k-1, 2k}}{\sqrt{2}}, \quad (62)$$

which we use in Fig. 3, where we show both thermalizing and non-thermalizing behaviors. In contrast to the situation here, for \mathfrak{L}_1 (dual-unitarity) the expectation values

spatial-temporal correlation functions are solvable and non-vanishing, while all dual-unitary circuits and their \mathfrak{L}_2 generalization have vanishing spatial-temporal correlations except on a few lines. Unfortunately, to date, we have not yet been able to find a nontrivial unitary gate satisfying this condition, due to the computational difficulty of solving this equation. We leave this possibility as an open direction for the future.

ACKNOWLEDGEMENTS

We thank Ignacio Cirac, Katja Klobas, Bruno Bertini and Alessandro Foligno for fruitful discussions. PK is supported by the Alexander von Humboldt Foundation.

Appendix A: A more general parametrization of dual-unitarity and hierarchy gates based on finite groups

In this appendix we give a further generalization of the parametrization of dual-unitarity and hierarchy gates presented in Sec. II A, based on projective representations of finite groups. Let G be a finite group and let Γ be an irreducible, unitary finite dimensional (with dimension D) projective representation of G , i.e. $\Gamma_a^\dagger = \Gamma_{a^{-1}}, \forall a \in G$ and

$$\Gamma_a \Gamma_b = \phi(a, b) \Gamma_{ab}, \quad \forall a, b \in G, \quad (\text{A1})$$

where $\phi(a, b)$ is a 2-cocycle of G , i.e.

$$\phi(a, b) \phi(ab, c) = \phi(b, c) \phi(a, bc), \quad \forall a, b, c \in G. \quad (\text{A2})$$

We further require that Γ satisfies a trace condition

$$\text{Tr}[\Gamma_a] = D \delta_{a,e}, \quad \forall a \in G, \quad (\text{A3})$$

where e is the unit of G . The irreducibility of Γ implies that $\{\Gamma_a\}_{a \in G}$ spans the matrix algebra $M_D(\mathbb{C})$, therefore, $\{\Gamma_a\}_{a \in G}$ is an orthonormal basis of $M_D(\mathbb{C})$ with trace normalization $\text{Tr}[\Gamma_a^\dagger \Gamma_b] = D \delta_{ab}, \forall a, b \in G$.

We use Eq. (9) again for the parametrization of 2-qudit unitary gate u , but now u_0 is defined as

$$u_0 = \sum_{a \in G} \theta_a |\psi_a\rangle \langle \psi_a|, \quad (\text{A4})$$

where $\{\theta_a\}_{a \in G}$ is a collection of $U(1)$ phases, and $\{|\psi_a\rangle\}_{a \in G}$ is an orthonormal basis for the 2-qudit Hilbert space $(\mathbb{C}^D)^2$ defined as

$$|\psi_a\rangle \equiv \frac{1}{\sqrt{D}} \sum_{1 \leq i, j \leq D} (\Gamma_a)_{ij}^* |i\rangle \otimes |j\rangle, \quad (\text{A5})$$

We proceed to investigate conditions on the parameters $\{\theta_a\}_{a \in G}$ for u to be a dual-unitary gate. After a space-time reshuffling of indices defined in Eq. (6), we have $\tilde{u} = (v_4^T \otimes v_2) \tilde{u}_0 (v_3 \otimes v_1^T)$, where

$$\tilde{u}_0 = \frac{1}{D} \sum_{a \in G} \theta_a \Gamma_a \otimes \Gamma_a^*. \quad (\text{A6})$$

Then the unitarity condition (7) on \tilde{u} is equivalent to

$$\sum_{a, b \in G} \theta_a \theta_b^* \Gamma_a \Gamma_b^\dagger \otimes \Gamma_a^* \Gamma_b^T = D^2 \Gamma_e \otimes \Gamma_e. \quad (\text{A7})$$

We simplify Eq. (A7) further with Eq. (A1) and, using the fact that $\{\Gamma_a\}_{a \in G}$ forms a basis of the matrix algebra $M_D(\mathbb{C})$, we obtain

$$\sum_{b \in G} \theta_{ab} \theta_b^* = D^2 \delta_{a,e}, \quad \forall a \in G. \quad (\text{A8})$$

Note that Eq. (A8) does not depend on the cocycle $\phi(a, b)$, only on the structure of the group G . Nevertheless, not all projective representations satisfy the trace condition (A3), and the 2-cocycle has to be chosen carefully to allow for such a projective representation.

As a specific example, consider the Abelian group $G = \mathbb{Z}_k^{\times 2n}$, where group elements are denoted as $a = (a_1, a_2, \dots, a_{2n}), 0 \leq a_j \leq k-1$, with multiplication rule $(a_1, \dots, a_{2n})(b_1, \dots, b_{2n}) = (a_1 + b_1, \dots, a_{2n} + b_{2n})$ (where all additions are modulo k), and the 2-cocycle is given by

$$\phi(a, b) = \omega^{-\sum_{1 \leq i < j \leq 2n} b_i a_j}, \quad (\text{A9})$$

where ω is a k -th root of unity. The projective representation Γ is defined as

$$\Gamma_a = \gamma_1^{a_1} \gamma_2^{a_2} \dots \gamma_{2n}^{a_{2n}}, \quad (\text{A10})$$

where $\gamma_1, \gamma_2, \dots, \gamma_{2n}$ are $D \times D$ matrices with $D = k^n$ satisfying

$$\begin{aligned} \gamma_j^k &= 1, \quad 1 \leq j \leq 2n \\ \gamma_i \gamma_j &= \omega \gamma_j \gamma_i, \quad 1 \leq i < j \leq 2n. \end{aligned} \quad (\text{A11})$$

The parametrization presented in Sec. II A corresponds to the special case $n = 1$.

Appendix B: The parametrization of the Hierarchical gates in higher dimensions

In this appendix, we provide further details about deriving Eq. (27). In particular, inserting Eqs. (9) and (10) into the first equation of (20) with $v_3 = v_4 = I_D$, we obtain

$$\begin{aligned}
& \sum_{a,b,c,d} \theta_{p_b,q_b}^* \theta_{p_a,q_a} \theta_{p_d,q_d}^* \theta_{p_c,q_c} \tau_{p_b,q_b}^\dagger \tau_{p_a,q_a} \otimes \tau_{p_d,q_d}^\dagger v_1^* \tau_{p_b,q_b}^T \tau_{p_a,q_a}^* v_1^T \tau_{p_c,q_c} \otimes \tau_{p_d,q_d}^T \tau_{p_c,q_c}^* \\
&= D^2 \sum_{c,d} \theta_{p_d,q_d}^* \theta_{p_c,q_c} I_D \otimes \tau_{p_d,q_d}^\dagger \tau_{p_c,q_c} \otimes \tau_{p_d,q_d}^T \tau_{p_c,q_c}^*. \tag{B1}
\end{aligned}$$

With the help of Eq. (16), this can be simplified to

$$\begin{aligned}
& \sum_{a,b,c,d} \omega^{qdpc} \theta_{p_b,q_b}^* \theta_{p_a,q_a} \theta_{p_d,q_d}^* \theta_{p_c,q_c} \tau_{p_a-p_b,q_a-q_b} \otimes \tau_{-p_d,-q_d} v_1^* \tau_{p_a-p_b,q_b-q_a} v_1^T \tau_{p_c,q_c} \otimes \tau_{p_c-p_d,q_d-q_c} \\
&= D^2 \sum_{c,d} \theta_{p_d,q_d}^* \theta_{p_c,q_c} I_D \otimes \tau_{p_c-p_d,q_c-q_d} \otimes \tau_{p_c-p_d,q_d-q_c}. \tag{B2}
\end{aligned}$$

We can relabel the dummy variables $p_a = p_b + k, q_a = q_b + l, p_c = p_d + s, q_c = q_d + t$ so that the independent Clifford group matrix is separated as

$$\begin{aligned}
& \sum_{k,l} \left(\sum_b \theta_{p_b,q_b}^* \theta_{p_b+k,q_b+l} \right) \tau_{k,l} \otimes \sum_{s,t} \left(\sum_d \theta_{p_d,q_d}^* \theta_{p_d+s,q_d+t} \tau_{p_d,q_d}^\dagger v_1^* \tau_{k,-l} v_1^T \tau_{p_d,q_d} \right) \tau_{s,t} \otimes \tau_{s,-t} \\
&= D^2 \sum_{s,t} \sum_d \theta_{p_d,q_d}^* \theta_{p_d+s,q_d+t} I_D \otimes \tau_{s,t} \otimes \tau_{s,-t}, \tag{B3}
\end{aligned}$$

where we have used the equality $\tau_{p_c,q_c} = \tau_{p_d,q_d} \tau_{s,t} \omega^{-qd s}$.

Note that Eq. (B3) is automatically satisfied for $(k, l) = (0, 0)$. Therefore, for $\forall (k, l) \neq 0$, the left hand side of Eq. (B3) must vanish, namely, either $\sum_b \theta_{p_b,q_b}^* \theta_{p_b+k,q_b+l} = 0$ or $\sum_d \theta_{p_d,q_d}^* \theta_{p_d+s,q_d+t} \tau_{p_d,q_d}^\dagger v_1^* \tau_{k,-l} v_1^T \tau_{p_d,q_d} = 0$, which gives the first line of Eq. (27) in the main text. The second line of Eq. (27) containing v_2 simplifies in a similar way using the second equation of (20).

The derivation of the \mathfrak{L}_3 condition follows exactly same procedure as above but may involve lots of tedious calculations. Here we just skip these details and give the result directly. With the parametrization method using Clifford group, Eq. (31) is equivalent to

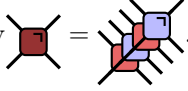
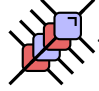
$$\begin{aligned}
& \left(\sum_{p_b,q_b} \theta_{p_b+s_a,q_b+t_a} \theta_{p_b,q_b}^* \right) \left(\sum_{p_d,q_d} \theta_{p_d+s_c,q_d+t_c} \theta_{p_d,q_d}^* \tau_{p_d,q_d}^\dagger v_1^* \tau_{s_a,-t_a} v_1^T \tau_{p_d,q_d} \right) \\
& \times \left(\sum_{p_f,q_f} \theta_{p_f+s_e,q_f+t_e} \theta_{p_f,q_f}^* \tau_{p_f,q_f}^\dagger v_1^* \tau_{s_c,-t_c} v_1^T \tau_{p_f,q_f} \right) = 0 \quad \text{for } \forall (s_a, t_a) \neq (0, 0). \tag{B4}
\end{aligned}$$

Appendix C: Proof of Eq. (30)

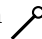
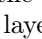
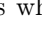
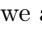
To prove this implication, we introduce the definitions

$$A = \begin{array}{c} \text{---} \\ \diagup \quad \diagdown \\ \text{---} \end{array} - \begin{array}{c} \text{---} \\ \diagdown \quad \diagup \\ \text{---} \end{array}, B = \begin{array}{c} \text{---} \\ \diagup \quad \diagdown \\ \text{---} \end{array} - \begin{array}{c} \text{---} \\ \diagdown \quad \diagup \\ \text{---} \end{array}. \quad (\text{C1})$$

By proving $\text{Tr}A^\dagger A = \text{Tr}B^\dagger B$, we establish that if A vanishes, then B also vanishes. This can be proved graphically. To this end, we introduce a four-folded gate given by

given by  = . The first term of $\text{Tr}A^\dagger A$ is

$$\text{Tr} \left(\begin{array}{c} \text{---} \\ \diagup \quad \diagdown \\ \text{---} \end{array} \right)^\dagger \left(\begin{array}{c} \text{---} \\ \diagup \quad \diagdown \\ \text{---} \end{array} \right) = \begin{array}{c} \text{---} \\ \diagup \quad \diagdown \\ \text{---} \end{array} \quad (\text{C2})$$

The contraction  represents a contraction between the same leg from the first and second layer as well as the third and fourth layer. Similarly, the contraction  represents a contraction between the first and fourth layer as well as second and third layer. It is worth noting that the result remains the same if we exchange the second and fourth layers while simultaneously exchange  and . Therefore, we arrive at

$$\text{Tr} \left(\begin{array}{c} \text{---} \\ \diagup \quad \diagdown \\ \text{---} \end{array} \right)^\dagger \left(\begin{array}{c} \text{---} \\ \diagup \quad \diagdown \\ \text{---} \end{array} \right) = \begin{array}{c} \text{---} \\ \diagup \quad \diagdown \\ \text{---} \end{array} = \begin{array}{c} \text{---} \\ \diagup \quad \diagdown \\ \text{---} \end{array} \quad (\text{C3})$$

The R.H.S. just corresponds to the first term in $\text{Tr}B^\dagger B$. By performing similar calculations, we can establish the agreement between each term of $\text{Tr}A^\dagger A$ and $\text{Tr}B^\dagger B$.

Appendix D: Numerical values of the parameters of the gates

In Fig. 1(b) and Fig. 3, we choose single site operators as $v_3 = v_4 = I$, $v_1 = v_2 = v$. The parameters for $v = e^{i\theta(\cos\theta\sigma_z + \sin\theta\cos\phi\sigma_x + \sin\theta\sin\phi\sigma_y)}$ are listed in Table I.

r	θ	ϕ	r	θ	ϕ	r	θ	ϕ
1.24056	0.84429	-0.4764	1	0.99788	3	$\frac{\pi}{4}$	$\frac{\pi}{2}$	0

TABLE I. The left set of parameters is the one for Fig. 1(b) and the blue line in Fig. 3. The middle set corresponds to the green line in Fig. 3 and the right set corresponds to the red line in Fig. 3.

-
- [1] A. J. Daley, C. Kollath, U. Schollwöck, and G. Vidal, Time-dependent density-matrix renormalization-group using adaptive effective hilbert spaces, *Journal of Statistical Mechanics: Theory and Experiment* **2004**, P04005 (2004).
- [2] N. Schuch, M. M. Wolf, F. Verstraete, and J. I. Cirac, Entropy scaling and simulability by matrix product states, *Phys. Rev. Lett.* **100**, 030504 (2008).
- [3] M. Ljubotina, L. Zadnik, and T. c. v. Prosen, Ballistic spin transport in a periodically driven integrable quantum system, *Phys. Rev. Lett.* **122**, 150605 (2019).
- [4] M. P. Fisher, V. Khemani, A. Nahum, and S. Vijay, Random quantum circuits, *Annual Review of Condensed Matter Physics* **14**, 335 (2023).
- [5] B. Bertini, P. Kos, and T. Prosen, Exact correlation functions for dual-unitary lattice models in 1+1 dimensions, *Phys. Rev. Lett.* **123**, 210601 (2019).
- [6] L. Piroli, B. Bertini, J. I. Cirac, and T. Prosen, Exact dynamics in dual-unitary quantum circuits, *Phys. Rev. B* **101**, 094304 (2020).
- [7] B. Bertini, P. Kos, and T. Prosen, Exact spectral form factor in a minimal model of many-body quantum chaos, *Phys. Rev. Lett.* **121**, 264101 (2018).
- [8] B. Bertini, P. Kos, and T. Prosen, Random matrix spectral form factor of dual-unitary quantum circuits, *Communications in Mathematical Physics* (2021).
- [9] B. Bertini, P. Kos, and T. Prosen, Entanglement spreading in a minimal model of maximal many-body quantum chaos, *Phys. Rev. X* **9**, 021033 (2019).
- [10] B. Bertini, P. Kos, and T. Prosen, Operator Entanglement in Local Quantum Circuits I: Chaotic Dual-Unitary Circuits, *SciPost Phys.* **8**, 67 (2020).
- [11] S. Gopalakrishnan and A. Lamacraft, Unitary circuits of finite depth and infinite width from quantum channels, *Phys. Rev. B* **100**, 064309 (2019).
- [12] P. W. Claeys and A. Lamacraft, Maximum velocity quantum circuits, *Phys. Rev. Res.* **2**, 033032 (2020).
- [13] B. Bertini and L. Piroli, Scrambling in random unitary circuits: Exact results, *Phys. Rev. B* **102**, 064305 (2020).
- [14] I. Reid and B. Bertini, Entanglement barriers in dual-unitary circuits, *Phys. Rev. B* **104**, 014301 (2021).
- [15] T. Zhou and A. W. Harrow, Maximal entanglement velocity implies dual unitarity, *Physical Review B* **106**, 10.1103/physrevb.106.1201104 (2022).
- [16] W. W. Ho and S. Choi, Exact emergent quantum state designs from quantum chaotic dynamics, *Phys. Rev. Lett.* **128**, 060601 (2022).
- [17] P. W. Claeys and A. Lamacraft, Emergent quantum state designs and biunitarity in dual-unitary circuit dynamics, *Quantum* **6**, 738 (2022).
- [18] M. Ippoliti and W. W. Ho, Dynamical purification and the emergence of quantum state designs from the pro-

- jected ensemble, [arXiv:2204.13657](https://arxiv.org/abs/2204.13657) (2022).
- [19] F. Fritzsche and T. Prosen, Eigenstate thermalization in dual-unitary quantum circuits: Asymptotics of spectral functions, *Phys. Rev. E* **103**, 062133 (2021).
- [20] A. Lerose, M. Sonner, and D. A. Abanin, Influence matrix approach to many-body Floquet dynamics, *Phys. Rev. X* **11**, 021040 (2021).
- [21] G. Giudice, G. Giudici, M. Sonner, J. Thoenness, A. Lerose, D. A. Abanin, and L. Piroli, Temporal entanglement, quasiparticles, and the role of interactions, *Phys. Rev. Lett.* **128**, 220401 (2022).
- [22] A. Foligno, T. Zhou, and B. Bertini, Temporal entanglement in chaotic quantum circuits (2023), [arXiv:2302.08502](https://arxiv.org/abs/2302.08502) [quant-ph].
- [23] M. Ippoliti and V. Khemani, Postselection-free entanglement dynamics via spacetime duality, *Phys. Rev. Lett.* **126**, 060501 (2021).
- [24] M. Ippoliti, T. Rakovszky, and V. Khemani, Fractal, logarithmic, and volume-law entangled nonthermal steady states via spacetime duality, *Phys. Rev. X* **12**, 011045 (2022).
- [25] T.-C. Lu and T. Grover, Spacetime duality between localization transitions and measurement-induced transitions, *PRX Quantum* **2**, 040319 (2021).
- [26] R. Suzuki, K. Mitarai, and K. Fujii, Computational power of one-and two-dimensional dual-unitary quantum circuits, *Quantum* **6**, 631 (2022).
- [27] E. Chertkov, J. Bohnet, D. Francois, J. Gaebler, D. Gresh, A. Hankin, K. Lee, D. Hayes, B. Neyenhuis, R. Stutz, A. C. Potter, and M. Foss-Feig, Holographic dynamics simulations with a trapped-ion quantum computer, *Nature Physics* **18**, 1074 (2022).
- [28] X. Mi, P. Roushan, C. Quintana, S. Mandrà, J. Marshall, C. Neill, F. Arute, K. Arya, J. Atalaya, R. Babush, J. C. Bardin, R. Barends, J. Basso, A. Bengtsson, S. Boixo, A. Bourassa, M. Broughton, B. B. Buckley, D. A. Buell, B. Burkett, N. Bushnell, Z. Chen, B. Chiaro, R. Collins, W. Courtney, S. Demura, A. R. Derk, A. Dunsworth, D. Eppens, C. Erickson, E. Farhi, A. G. Fowler, B. Foxen, C. Gidney, M. Giustina, J. A. Gross, M. P. Harrigan, S. D. Harrington, J. Hilton, A. Ho, S. Hong, T. Huang, W. J. Huggins, L. B. Ioffe, S. V. Isakov, E. Jeffrey, Z. Jiang, C. Jones, D. Kafri, J. Kelly, S. Kim, A. Kitaev, P. V. Klimov, A. N. Korotkov, F. Kostritsa, D. Landhuis, P. Laptev, E. Lucero, O. Martin, J. R. McClean, T. McCourt, M. McEwen, A. Megrant, K. C. Miao, M. Mohseni, S. Montazeri, W. Mruczkiewicz, J. Mutus, O. Naaman, M. Neeley, M. Newman, M. Y. Niu, T. E. O'Brien, A. Opremcak, E. Ostby, B. Pato, A. Petukhov, N. Redd, N. C. Rubin, D. Sank, K. J. Satzinger, V. Shvarts, D. Strain, M. Szalay, M. D. Trevithick, B. Villalonga, T. White, Z. J. Yao, P. Yeh, A. Zalcman, H. Neven, I. Aleiner, K. Kechedzhi, V. Smelyanskiy, and Y. Chen, Information scrambling in quantum circuits, *Science* **374**, 1479 (2021).
- [29] S. A. Rather, S. Aravinda, and A. Lakshminarayan, Creating ensembles of dual unitary and maximally entangling quantum evolutions, *Phys. Rev. Lett.* **125**, 070501 (2020).
- [30] B. Gutkin, P. Braun, M. Akila, D. Waltner, and T. Guhr, Exact local correlations in kicked chains, *Phys. Rev. B* **102**, 174307 (2020).
- [31] P. W. Claeys and A. Lamacraft, Ergodic and nonergodic dual-unitary quantum circuits with arbitrary local Hilbert space dimension, *Phys. Rev. Lett.* **126**, 100603 (2021).
- [32] S. Aravinda, S. A. Rather, and A. Lakshminarayan, From dual-unitary to quantum Bernoulli circuits: Role of the entangling power in constructing a quantum ergodic hierarchy, *Phys. Rev. Research* **3**, 043034 (2021).
- [33] T. Prosen, Many-body quantum chaos and dual-unitarity round-a-face, *Chaos: An Interdisciplinary Journal of Nonlinear Science* **31**, 093101 (2021).
- [34] M. Borsi and B. Pozsgay, Construction and the ergodicity properties of dual unitary quantum circuits, *Phys. Rev. B* **106**, 014302 (2022).
- [35] M. Mestyán, B. Pozsgay, and I. M. Wanless, Multi-directional unitarity and maximal entanglement in spatially symmetric quantum states (2022), [arXiv:2210.13017](https://arxiv.org/abs/2210.13017) [quant-ph].
- [36] P. W. Claeys, A. Lamacraft, and J. Vicary, From dual-unitary to biunitary: a 2-categorical model for exactly-solvable many-body quantum dynamics (2023), [arXiv:2302.07280](https://arxiv.org/abs/2302.07280) [quant-ph].
- [37] P. Kos, B. Bertini, and T. Prosen, Correlations in perturbed dual-unitary circuits: Efficient path-integral formula, *Phys. Rev. X* **11**, 011022 (2021).
- [38] M. A. Rampp, R. Moessner, and P. W. Claeys, From dual unitarity to generic quantum operator spreading, *Phys. Rev. Lett.* **130**, 130402 (2023).
- [39] C. Jonay, V. Khemani, and M. Ippoliti, Triunitary quantum circuits, *Phys. Rev. Research* **3**, 043046 (2021).
- [40] R. M. Milbradt, L. Scheller, C. Åkhus, and C. B. Mendl, Ternary unitary quantum lattice models and circuits in $2 + 1$ dimensions, *Phys. Rev. Lett.* **130**, 090601 (2023).
- [41] Y. Kasim and T. Prosen, Dual unitary circuits in random geometries, *Journal of Physics A: Mathematical and Theoretical* **56**, 025003 (2023).
- [42] L. Masanes, Discrete holography in dual-unitary circuits (2023), [arXiv:2301.02825](https://arxiv.org/abs/2301.02825) [hep-th].
- [43] P. Kos and G. Styliaris, Circuits of space and time quantum channels, *Quantum* **7**, 1020 (2023).
- [44] A. Christopoulos, A. D. Luca, D. L. Kovrizhin, and T. Prosen, Dual symplectic classical circuits: An exactly solvable model of many-body chaos (2023), [arXiv:2307.01786](https://arxiv.org/abs/2307.01786) [nlin.CD].
- [45] J. E. Tyson, Operator-schmidt decompositions and the fourier transform, with applications to the operator-schmidt numbers of unitaries, *Journal of Physics A: Mathematical and General* **36**, 10101 (2003).
- [46] M. Medenjak, K. Klobas, and T. Prosen, Diffusion in deterministic interacting lattice systems, *Physical Review Letters* **119**, 10.1103/physrevlett.119.110603 (2017).
- [47] K. Klobas, M. Medenjak, T. Prosen, and M. Vanicat, Time-dependent matrix product ansatz for interacting reversible dynamics, *Communications in Mathematical Physics* **371**, 651 (2019).
- [48] K. Klobas and B. Bertini, Exact relaxation to gibbs and non-equilibrium steady states in the quantum cellular automaton rule 54, *SciPost Physics* **11**, 10.21468/scipostphys.11.6.106 (2021).
- [49] K. Klobas, C. D. Fazio, and J. P. Garrahan, Exact "hydrophobicity" in deterministic circuits: dynamical fluctuations in the floquet-east model (2023), [arXiv:2305.07423](https://arxiv.org/abs/2305.07423) [cond-mat.stat-mech].
- [50] B. Bertini, P. Kos, and T. Prosen, Localised dynamics in the floquet quantum east model (2023), [arXiv:2306.12467](https://arxiv.org/abs/2306.12467) [cond-mat.stat-mech].

- [51] K. Klobas, B. Bertini, and L. Piroli, Exact thermalization dynamics in the “rule 54” quantum cellular automaton, [Phys. Rev. Lett. **126**, 160602 \(2021\)](#).
- [52] A. Foligno, K. Klobas, and B. Bertini, In preparation.